containing 1.03 g of *cis*-Pt(CH₃)₂Q₂ (2.05 mmol) and 15 ml of acetone. The tube was sealed and shaken at room temperature for 1 week. No polymer precipitated. The tube was opened, and the solution was filtered and then evaporated to a brown oil, which, from its nmr spectrum (dissolved in chloroform), contained *cis*-Pt(CH₃)₂Q₂ and *cis*- and *trans*-Pt(CH₃)(-C≡CCF₃)Q₂. The oil was dissolved in ether, and pentane was added to precipitate out Pt(CH₃)₂Q₂ and *cis*-Pt(CH₃)(-C≡CCF₃)Q₂. The ether–pentane solution was decanted from the precipitated oil and then evaporated to dryness. The resultant yellow-brown oil, consisting mainly of *trans*-Pt(CH₃)(-C≡CCF₃)Q₂, was dissolved in pentane and then chromatographed on Florisil, using pentane and then pentane containing increasing proportions of diethyl ether to elute the column. A colorless oil was obtained on evaporation of the appropriate fractions and solidified to a white solid on standing. A total of 0.05 g was obtained as pure *trans*-Pt(CH₃)(-C≡CCF₃)Q₂.

cis-Pt(CH₃)₂{As(CH₃)₂(C₆H₅)}₂ with CF₃C≡CH in Benzene (**Reaction 18**).—*cis*-Pt(CH₃)₂{As(CH₃)₂(C₆H₅)}₂ (0.386 g, 0.7 mmol) in 3 ml of benzene was shaken with 6 mmol of CF₃C≡CH in a sealed Carius tube. Within 12 hr, a small amount of polymer had precipitated, and the initially colorless solution had turned pale brown. After 10 days the tube was opened, 0.145 g polymer was filtered off, and the filtrate was evaporated. The residue consisted of an orange mixture of a solid with an oil. On addition of pentane, the oil dissolved, but most of the solid remained (0.11 g). Recrystallization of this solid from ether–pentane gave 0.05 g of *trans*-Pt(-C≡CCF₃)₂{As(CH₃)₂(C₆H₅)}₂ as a white solid.

CONTRIBUTION FROM THE DEPARTMENT OF CHEMISTRY,
UNIVERSITY OF HAWAII, HONOLULU, HAWAII 96822

Halide-Bridged Electrode Reactions of Platinum Complexes Containing Unsaturated Ligands
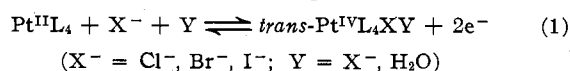
BY CHIU-NAN LAI AND ARTHUR T. HUBBARD*

Electrochemical interconversion of complexes of Pt(II) and Pt(IV) is accelerated by the presence of halide ions and halogen ligands. The influence of the halogens is consistent with the suggestion that halide acts as a bridging group between the reactant complex and the electrode surface or compact double layer. In particular, oxidation of Pt(II) may involve the transfer of electron density from filled orbitals of the complex, such as $a_{1g}(\sigma^*)$ [$5d_{z^2}$], through unfilled orbitals such as nd_{z^2} of an intervening halide ion to certain unfilled orbitals of the compact layer or the electrode surface. Or, oxidation may proceed through orbitals such as nd_{z^2} of a halide ligand of the Pt(II) complex rather than through a free halide ion. Similarly, reduction of Pt(IV) complexes, for instance those of D_{4h} symmetry such as $Pt^{IV}L_4X_2$, may proceed through interaction of a low-energy unfilled orbital of Pt(IV), such as $a_{1g}(\sigma^*)$, with filled orbitals of the compact layer or the electrode surface by way of the unfilled nd_{z^2} orbital of a bridging halide ligand. Pt(II) complexes containing unsaturated ligands such as CN^- or SCN^- are less rapidly oxidized than their saturated analogs. Evidence is presented that unsaturated ligands having suitable π^* orbitals stabilize the particular orbitals from which electron density is removed in the rate-limiting step. Pt(IV) complexes having a CN^- ligand situated trans to a lone halide ligand are reduced with difficulty, whereas complexes having a trans pair of halide ligands react readily; this trend is consistent with stabilization of the leaving trans axis and destabilization of the interaction between the bridging ligand and the electrode surface due to d–π^* back-bonding between Pt(IV) and the unsaturated ligand.

Introduction

Electrochemical interconversion of platinum(II) and -(IV) complexes is stereospecific.[1-4] Oxidation of Pt(II) complexes in the presence of halide ions proceeds readily to give *trans*-dihaloplatinum(IV) or *trans*-haloaquoplatinum(IV) complexes,[2] *i.e.*

$$Pt^{II}L_4 + X^- + Y \rightleftharpoons trans\text{-}Pt^{IV}L_4XY + 2e^- \qquad (1)$$

$$(X^- = Cl^-, Br^-, I^-; \; Y = X^-, H_2O)$$

Detailed kinetic characterization of the reactions with consideration of the charge and structure of the electrical double layer[4] as well as of the reactant complex[2] has led to the axial ligand-bridge mechanism, according to which electron transfer proceeds through an adsorbed-halide bridge located between the electrode and the platinum complex in the transition state,[1-4] *i.e.*, eq 2.

When halide is present as a ligand but not as the free ion, the oxidation of Pt(II) is thought to proceed through an equatorially ligand-bridged transition state,[2] *i.e.*, eq 3.

Reduction of Pt(IV) complexes appears to follow eq 1–3, traversing the equations in the opposite direction. Reduction of a given Pt(IV) complex may not regenerate the Pt(II) starting material, in that removal of a trans axis other than the one added by oxidation may occur. In fact, parallel reduction to a mixture of Pt(II) products sometimes takes place when more than one potential ligand bridge is present in the Pt(IV) coordination sphere.[5]

Pt(II) complexes containing unsaturated ligands, for instance CN^-, SCN^-, and aromatic amines, appear to follow eq 1–3 but react more slowly than complexes of similar charge and structure containing only saturated ligands. The present studies demonstrate the influence of unsaturated ligands on Pt(II) reactivity and attempt to explain the results in terms of molecular orbital theory. It appears possible, in turn, to use these results to establish certain general mechanistic details of
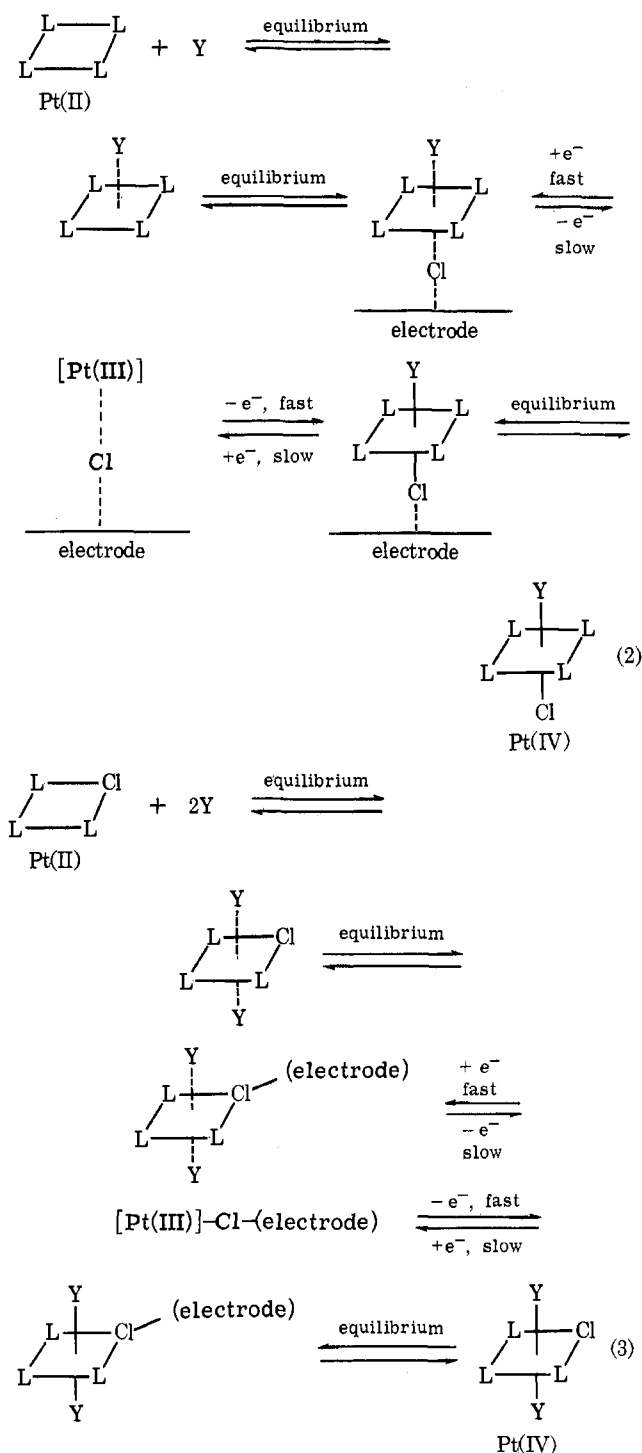
(1) W. R. Mason and R. C. Johnson, *J. Electroanal. Chem.*, **14**, 345 (1967).
(2) J. R. Cushing and A. T. Hubbard, *ibid.*, **23**, 183 (1969).
(3) A. L. Y. Lau and A. T. Hubbard, *ibid.*, **24**, 237 (1970).
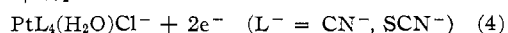(4) A. L. Y. Lau and A. T. Hubbard, *ibid.*, **33**, 77 (1971).

(5) R. F. Lane and A. T. Hubbard, University of Hawaii, unpublished experiments.

$$\text{(2)}$$

$$\text{(3)}$$

halide-accelerated interconversion of Pt(II) and Pt(IV) complexes of all types.

Results

Current–potential curves obtained for $Pt(CN)_4{}^{2-}$ at a polycrystalline platinum thin-layer electrode[2] in chloride solutions are shown in Figure 1. Oxidation of $Pt(CN)_4{}^{2-}$ takes place at very positive potentials just prior to the onset of chlorine evolution. Note that certain characteristics of the current–potential trace associated with background electrode behavior are altered by $Pt(CN)_4{}^{2-}$, particularly the hydrogen-de-

$$PtL_4{}^{2-} + Cl^- + H_2O \longrightarrow$$

$$PtL_4(H_2O)Cl^- + 2e^- \quad (L^- = CN^-, SCN^-) \quad (4)$$
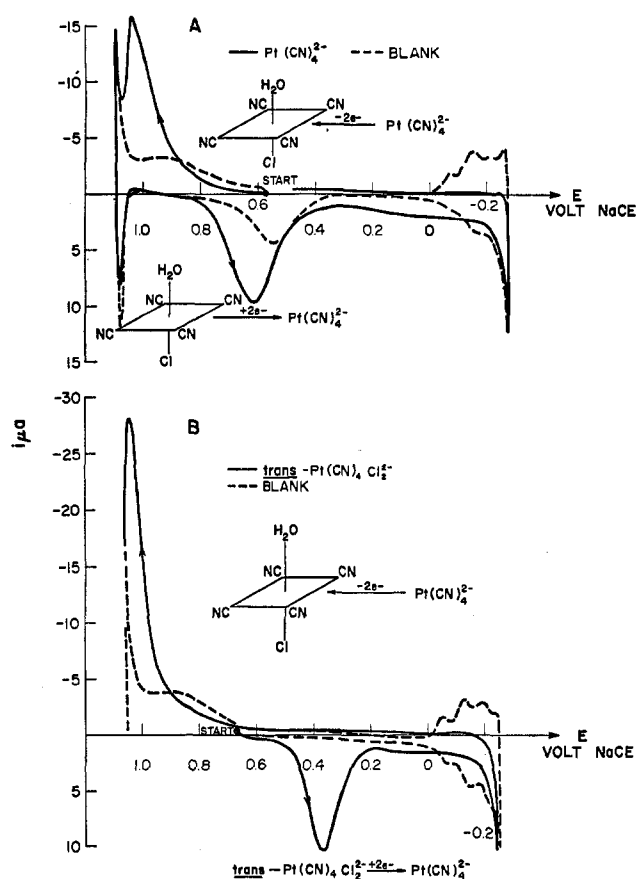
Figure 1.—Thin-layer current–potential curves for $Pt(CN)_4{}^{2-}$ and $Pt(CN)_4Cl_2{}^{2-}$: curve A, 1 mF $K_2Pt(CN)_4$ + 10 mF NaCl + 1 F HClO$_4$; curve B, 1 mF $K_2Pt(CN)_4Cl_2$ + 10 mF NaCl + 1 F HClO$_4$; blank curves, 10 mF NaCl + 1 F HClO$_4$. Experimental conditions: sweep rate, 2 mV/sec; thin-layer volume, 3.92 μl; platinum electrode area, 1.15 cm^2. Oxidation current is depicted as negative.

position peaks in the vicinity of zero on the potential axis; this is due to the release of a very small quantity of CN^- from the complex which subsequently becomes chemisorbed on the electrode surface. Reduction of $Pt(CN)_4Cl_2{}^{2-}$ proceeds irreversibly to yield $Pt(CN)_4{}^{2-}$; the anodic scan corresponds to the oxidation of $Pt(CN_4)^{2-}$ (Figure 1) in the presence of adsorbed CN^-. $Pt(SCN)_4{}^{2-}$ yields similar curves.

Introduction of two CN^- ligands into the coordination sphere of Pt(II) produces complexes which oxidize more slowly than their saturated analogs, as indicated by the current–potential curves shown in Figure 2. The difference in reactivity between cis and trans isomers is detectable but not striking. As with other neutral complexes studied earlier,[2–4] oxidation follows parallel paths to produce approximately equal amounts of the *trans*-dichloro- and -aquochloroplatinum(IV) complexes (eq 5 and 6; *cf.* eq 1 and 2). Addition of chloride to the solution linearly increases the proportion
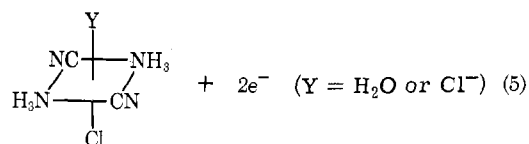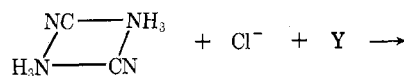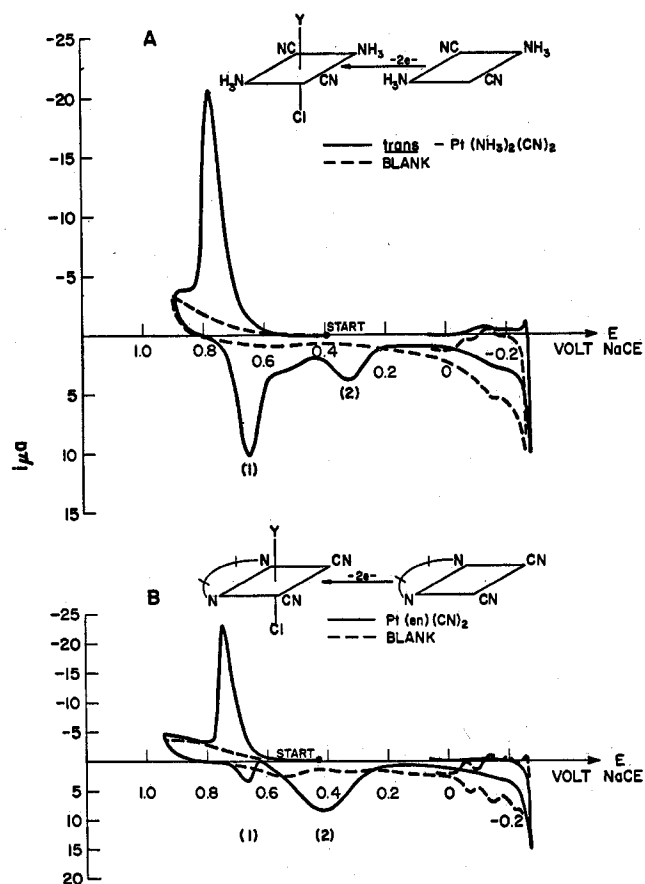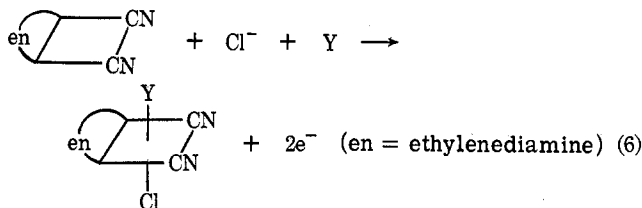
Figure 2.—Thin-layer current–potential curves for *trans*-Pt-$(NH_3)_2(CN)_2$ and $Pt(en)(CN)_2$: curve A, 1 mF *trans*-Pt$(NH_3)_2$-$(CN)_2$ + 10 mF NaCl + 1 F HClO$_4$; curve B, 1 mF Pt(en)-$(CN)_2$ + 10 mF NaCl + 1 F HClO$_4$; blank curves, 10 mF NaCl + 1 F HClO$_4$. Experimental conditions were as in Figure 1. Peaks labeled (1) are due to reduction of $Pt(NH_3)_2(CN)_2(H_2O)$-Cl^+ and $Pt(en)(CN)_2(H_2O)Cl^+$; peaks (2) are due to reduction of $Pt(NH_3)_2(CN)_2Cl_2$ and $Pt(en)(CN)_2Cl_2$.

$$en \begin{bmatrix} & CN \\ & CN \end{bmatrix} + Cl^- + Y \longrightarrow$$

$$en \begin{bmatrix} & Y \\ & CN \\ & CN \\ & Cl \end{bmatrix} + 2e^- \quad (en = ethylenediamine) \quad (6)$$

of the dichloroplatinum(IV) product,[2] presumably due to increased association between Pt(II) and Cl$^-$ prior to the rate-limiting electron-transfer step.

Coordination of CN$^-$ trans to a potential bridging chloride in Pt(IV) leads to complexes which reduce less rapidly than their saturated analogs as indicated by the current–potential curves for $Pt(CN)_5Cl^{2-}$, $Pt(en)_2$-$(CN)Cl^{2+}$, and $Pt(NH_3)_5Cl^{3+}$ in Figure 3. Ammonia, amines, and even chelons of multidentate amine chelates[5] do not prevent Pt(IV) reduction when present trans to the bridging ligand. Thus, the unreactivity of the CN$^-$ complexes is unique among all those studied to date. SCN$^-$ does not display this effect, apparently because SCN$^-$ is able to function as the bridging group, while Cl$^-$ serves as the leaving group. In keeping with this suggestion, $Pt(SCN)_6{}^{2-}$ is readily reduced whereas $Pt(CN)_6{}^{2-}$ is unreactive. $Pt(NH_3)_6{}^{4+}$ is also unreactive.[3] Current–potential data for all complexes discussed in this article appear in Table I.
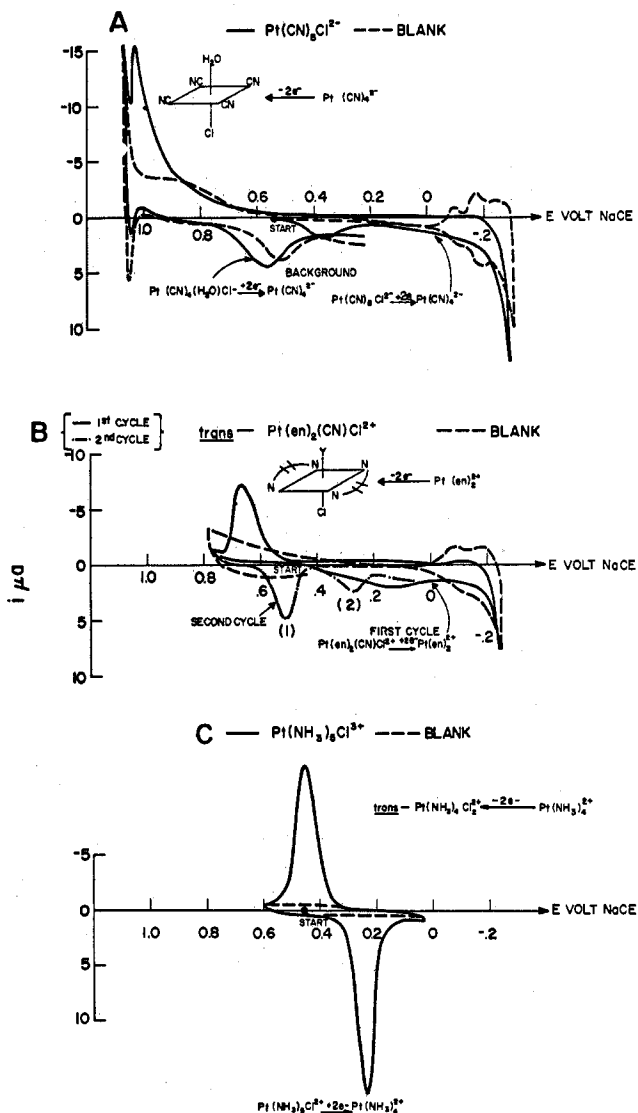

Figure 3.—Thin-layer current–potential curves for $Pt(CN)_5$-Cl^{2-}, *trans*-Pt(en)$_2$(CN)Cl^{2+}, and $Pt(NH_3)_5Cl^{3+}$: curve A, 1 mF $K_2Pt(CN)_5Cl$ + 10 mF NaCl + 1 F HClO$_4$; curve B, 1 mF *trans*-[Pt(en)$_2$(CN)Cl]Cl$_2$ + 1 F HClO$_4$; curve C, 1 mF [Pt(NH$_3$)$_5$Cl]-PO$_4$ + 10 mF NaCl + 1 F HClO$_4$; blank curves, same as above, but platinum complex omitted. Experimental conditions as in Figure 1. Peaks (1) and (2) of curve B are due to reduction of *trans*-Pt(en)$_2$(H$_2$O)Cl^{3+} and *trans*-Pt(en)$_2$Cl$_2{}^{2+}$, respectively.

Pt(II) complexes of aromatic amines such as pyridine and pyrazine (Figure 4) show normal reactivity toward oxidation by way of the axially ligand-bridged path (eq 3). Similarly, $Pt(NO_2)_4{}^{2-}$ is oxidized, although somewhat more slowly than $PtCl_4{}^{2-}$.

In a recent study it was reported that the electrode reactions of anionic platinum complexes typically proceed faster at electrodes containing chemisorbed species derived from solutions of alkenes, alkynes, CO, and I$^-$ than at clean electrodes, while cationic complexes react more slowly. Since it was expected that the unsaturated species studied in this work would chemisorb on the platinum electrode, a series of experiments was performed in which the current–potential curves for clean electrodes were compared with those obtained after the electrodes were rinsed with a dilute solution of the potential adsorbate and then thoroughly again with the pure electrolyte. The results (Figure 5) clearly

TABLE I

THIN-LAYER CURRENT-POTENTIAL DATA FOR Pt(IV)–Pt(II) COUPLES AT Pt ELECTRODES

A. Oxidation of Pt(II) Complexes

Reactant[a]	Product	^aE_p	^cE_p	$^aE_p - {^cE_p}$	$E°_{42}$	$1 - {^*\alpha_{23}}$	$^*k^\circ_{23}$	^aI_p, μA	$^*k^\circ_{23}f(E)$[g]
		(V vs. Na cc)							
Pt(CN)$_4$$^{2-}$	Pt(CN)$_4$(H$_2$O)Cl$^-$	1.04	0.62	0.42	0.72[d]	0.588	1.05×10^{-7}	12.75	1.03×10^{-5}
trans-Pt(NH$_3$)$_2$(CN)$_2$	trans-Pt(NH$_3$)$_2$(CN)$_2$(H$_2$O)Cl$^+$	0.78	0.65	0.13	0.57[d]	0.887	1.93×10^{-6}	19.25	1.94×10^{-2}
trans-Pt(NH$_3$)$_2$(CN)$_2$, 1 F NaCl	trans-Pt(NH$_3$)$_2$(CN)$_2$Cl$_2$	0.78	0.32	0.46	0.48[d]	0.887	7.60×10^{-9}	19.25	7.64×10^{-6}
Pt(en)(CN)$_2$	Pt(en)(CN)$_2$(H$_2$O)Cl$^+$	0.76	0.68	0.08	0.57[d]	0.968	2.04×10^{-7}	21	3.85×10^{-4}
Pt(en)(CN)$_2$, 1 F NaCl	Pt(en)(CN)$_2$Cl$_2$	0.76	0.42	0.34	0.341[i]	0.968	3.58×10^{-11}	21	6.76×10^{-8}
Pt(SCN)$_4$$^{2-}$	Unreactive								
trans-Pt(NH$_3$)$_2$(SCN)$_2$	trans-Pt(NH$_3$)$_2$(SCN)$_2$Cl$_2$	0.67	0.18	0.49	0.343[i]	0.476	3.01×10^{-7}	10.32	1.23×10^{-3}
Pt(NO$_2$)$_4$$^{2-}$	Pt(NO$_2$)$_4$(H$_2$O)Cl$^-$	0.81	0.42	0.39	0.576[j]	0.645	4.87×10^{-7}	14	7.42×10^{-3}
cis-Pt(NH$_3$)$_2$(NO$_2$)$_2$	trans-Pt(NH$_3$)$_2$(NO$_2$)$_2$(H$_2$O)Cl$^+$	0.66	0.56	0.10	0.408[i]	0.645	3.10×10^{-7}	14	4.72×10^{-5}
cis-Pt(NH$_3$)$_2$(NO$_2$)$_2$	trans-Pt(NH$_3$)$_2$(NO$_2$)$_2$Cl$_2$	0.66	0.37	0.29	0.408[i]	0.645	3.10×10^{-7}	14	4.72×10^{-3}
Pt(C$_2$H$_4$)Cl$_2$(H$_2$O)	Pt(C$_2$H$_4$)Cl$_4$(H$_2$O)	0.99	0.1	0.89	0.72[d]	0.738	8.59×10^{-8}	16	2.70×10^{-5}
Pt(py)$_4$$^{2+}$, 1 F H$_2SO_4$, 10 mF NaCl	Pt(py)$_4$Cl$_2$$^{2+}$	0.82	0.72	0.1	0.682[k]	0.645	5.40×10^{-6}	14	8.23×10^{-4}
Pt(NH$_3$)$_4$$^{2+}$	Pt(NH$_3$)$_4$Cl$_2$$^{2+}$	0.44	0.40	0.04	0.35[l]	[1.083][f]	$[6.53 \times 10^{-6}]$[f]	23.5	3.02×10^{-2}

B. Reduction of Pt(IV) Complexes

Reactant[a]	Product	^cE_p	^aE_p	$^cE_p - {^aE_p}$	$E°_{42}$	$^*\alpha_{43}$	$^*k^\circ_{43}$	^cI_p, μA	$^*k^\circ_{43}g(E)$[h]
		(V vs. Na cc)							
Pt(CN)$_6$$^{2-}$	Unreactive								
Pt(CN)$_5$Cl^{2-}	Pt(CN)$_4$$^{2-}$	b	1.03						
Pt(CN)$_4$Cl$_2$$^{2-}$	Pt(CN)$_4$$^{2-}$	0.37	1.04	-0.72	0.65[l]	0.461	8.16×10^{-7}	10	2.96×10^{-5}
trans-Pt(en)$_2$(CN)Cl^{2+}, 2 mF NaCl	Pt(en)$_2$$^{2+}$	b	0.66		0.23[l]	0.392	6.60×10^{-5}	8.5	1.40×10^{-3}
Pt(SCN)$_6$$^{2-}$, no Cl$^-$ in solution	Pt(SCN)$_4$$^{2-}$	0.02	b						
Pt(en)$_2$(SCN)Cl^{2+}	Pt(en)$_2$$^{2+}$	0.26	0.46	-0.20	0.31[e]	0.751	4.64×10^{-5}	16.3	1.62×10^{-2}
Pt(NO$_2$)$_4$Cl$_2$$^{2-}$, 2 mF NaCl	Pt(NO$_2$)$_4$$^{2-}$	0.26	0.80	-0.54	0.4[l]	0.484	9.26×10^{-6}	10.5	3.49×10^{-5}
trans-Pt(NH$_3$)$_4$Cl$_2$$^{2+}$	Pt(NH$_3$)$_4$$^{2+}$	0.40	0.465	-0.065	0.35[l]	[1.153][f]	$[2.87 \times 10^{-3}]$[f]	25	2.30×10^{1} [c]
Pt(NH$_3$)$_5$Cl^{3+}	Pt(NH$_3$)$_4$$^{2+}$	0.234	0.455	-0.221	0.282[e]	0.756	4.9×10^{-5}	16.4	1.77×10^{-2}

[a] In solution of 1 F HClO$_4$ + 10 mF NaCl except where otherwise indicated. [b] Reaction too slow to be measured. [c] Reaction rate too large for accurate measurement. [d] The method of obtaining the value will be discussed elsewhere in the text. [e] Value obtained by measuring the potential established by equimolar quantities of Pt(II) and Pt(IV) couples in 1 F NaCl. [f] Value is only approximate; the reaction is too fast for accurate measurement. [g] $f(E) \equiv \exp[((1 - {^*\alpha_{23}})F/RT)(E - E°_{42})]$. [h] $g(E) \equiv \exp[(- {^*\alpha_{43}}F/RT)(E - E°_{42})]$. [i] Yu. N. Kukushkin and S. Ch. Dkhara, *Russ. J. Inorg. Chem.,* **14,** 1483 (1969); I. I. Chernyaev, S. V. Zemskov, and B. V. Ptitsyn, *ibid.,* **10,** 1309 (1965). [j] Reference 2. [k] A. Davison, M. L. H. Green, and G. Wilkinson, *J. Chem. Soc.,* 3172 (1961). [l] R. N. Goldberg and L. G. Hepler, *Chem. Rev.,* **68,** 229 (1968).

TABLE II

SOURCES OF PLATINUM COMPOUNDS EMPLOYED IN THIS STUDY

Compd	Source or ref to prepn	Compd	Source or ref to prepn	Compd	Source or ref to prepn
[Pt(NH$_3$)$_4$]Cl$_2$	a	[Pt(py)$_4$]Cl$_2$	e	trans-[Pt(en)$_2$(CN)Cl]Cl$_2$	d
K$_2$Pt(CN)$_4$	a	trans-Pt(NH$_3$)$_2$(SCN)$_2$	c	[Pt(NH$_3$)$_5$Cl]Cl$_3$	i
cis-Pt(NH$_3$)$_2$(NO$_2$)$_2$	a	K$_2$Pt(SCN)$_4$	a	K$_2$Pt(CN)$_6$	h, j
Pt(en)(CN)$_2$	b, d	K$_2$Pt(CH$_2$=CH$_2$)Cl$_3$	f	trans-[Pt(en)$_2$(SCN)Cl](NO$_3$)$_2$	d
trans-Pt(NH$_3$)$_2$(CN)$_2$	c, d	trans-K$_2$Pt(CN)$_4$Cl$_2$	g, h	K$_2$Pt(SCN)$_6$	a
K$_2$Pt(NO$_2$)$_4$	a	K$_2$Pt(CN)$_5$Cl	h		

[a] K & K Laboratories, Inc., Plainview, N. Y. 11803. [b] I. B. Baranovskii and Yu. Ya. Kharitonov, *Dokl. Akad. Nauk SSSR, Ser. Khim.,* **169,** 805 (1966). [c] Yu. Ya. Kharitonov, O. N. Evstaf'eva, I. B. Baranovskii, and G. Ya. Mazo, *Russ. J. Inorg. Chem.,* **14,** 248 (1969). [d] Preparation described elsewhere in this article. [e] G. B. Kauffman, *Inorg. Syn.,* **7,** 251 (1963). [f] J. Chatt and M. L. Searle, *ibid.,* **5,** 214 (1957). [g] W. R. Mason, Jr., III, *Inorg. Chem.,* **9,** 1528 (1970). [h] We are indebted to Dr. Mason for providing us with a sample of this compound. [i] D. L. Swihart and W. R. Mason, Jr., III, *Inorg. Chem.,* **9,** 1749 (1970). [j] "Gmelin's Handbuch der anorganischen Chemie," Vol. 68D, Verlag Chemie, Weinheim/Bergstrasse, 1957, p 480 ff.
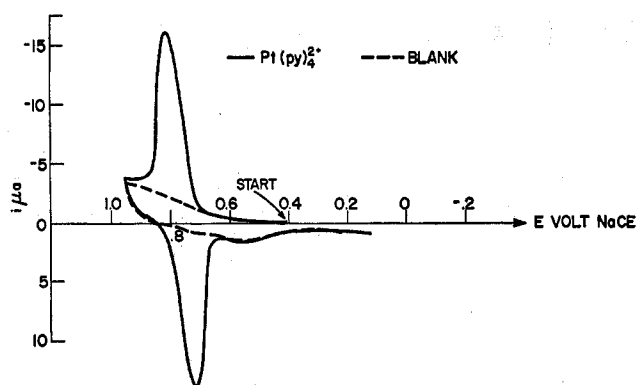
Figure 4.—Thin-layer current–potential curves for pyridine complexes of Pt(II) and Pt(IV): solid curve, 1 mF [Pt(py)$_4$]Cl$_2$ + 10 mF NaCl + HClO$_4$; broken curve, 10 mF NaCl + 1 F HClO$_4$. Experimental conditions as in Figure 1.
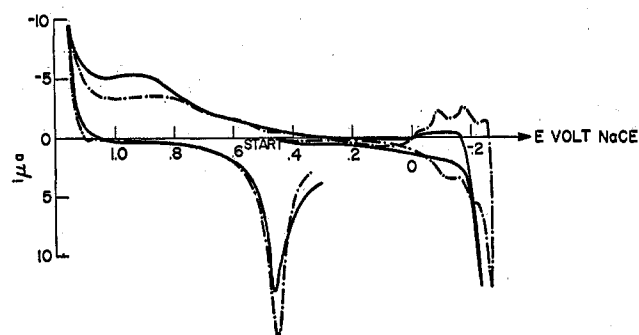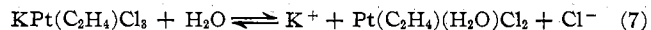

Figure 5.—Thin-layer current–potential: solid curve, CN-coated platinum electrode; broken curve, clean platinum electrode. Experimental conditions: sweep rate, 2 mV/sec; electrode area, 1.15 cm^2; thin-layer volume, 3.92 μl; supporting electrolyte, 1 F HClO$_4$. The electrode was pretreated as described in the Experimental Section except that prior to recording the solid curve the electrode was rinsed for 30 sec with 2 mF NaCN, followed by thorough rinsing with water and with the pure supporting electrolyte.

demonstrate that CN$^-$ and SCN$^-$ lead to chemisorption; note the disappearance of the hydrogen adsorption prewaves in the vicinity of 0 V and the appearance of a peak for oxidation of the adsorbed material in the vicinity of 1 V. The influence of pretreatment with CN$^-$ on the electrode reactions of representative platinum complexes is illustrated in Figure 6. Although the influence of surfactant is evident, it is not sufficiently striking to account for the observed unreactivity of CN$^-$ complexes.

Results obtained for Pt(C$_2$H$_4$)Cl$_3$$^-$ (Zeise's salt) are illustrated in Figure 7. Substitution of the Cl$^-$ ligand trans to ethylene accompanies dissolution in the solvent[6]

$$\text{KPt(C}_2\text{H}_4\text{)Cl}_3 + \text{H}_2\text{O} \rightleftharpoons \text{K}^+ + \text{Pt(C}_2\text{H}_4\text{)(H}_2\text{O)Cl}_2 + \text{Cl}^- \quad (7)$$

Ethylene released from the complex in trace amounts is chemisorbed on the electrode surface; the adsorbed material undoubtedly retards the oxidation of the complex somewhat.[4] Nevertheless, oxidation of Pt-(C$_2$H$_4$)(H$_2$O)Cl$_2$ is observed, although at rather positive potentials [$_a E_p$ = 0.96 V $vs.$ Na ce (sodium calomel electrode)]. Not only is the ethylenic complex less reactive than neutral complexes with saturated ligands such as cis- or trans-Pt(NH$_3$)$_2$Cl$_2$, but it reacts solely by

(6) S. J. Lokken and D. S. Martin, *Inorg. Chem.*, **2**, 562 (1963).
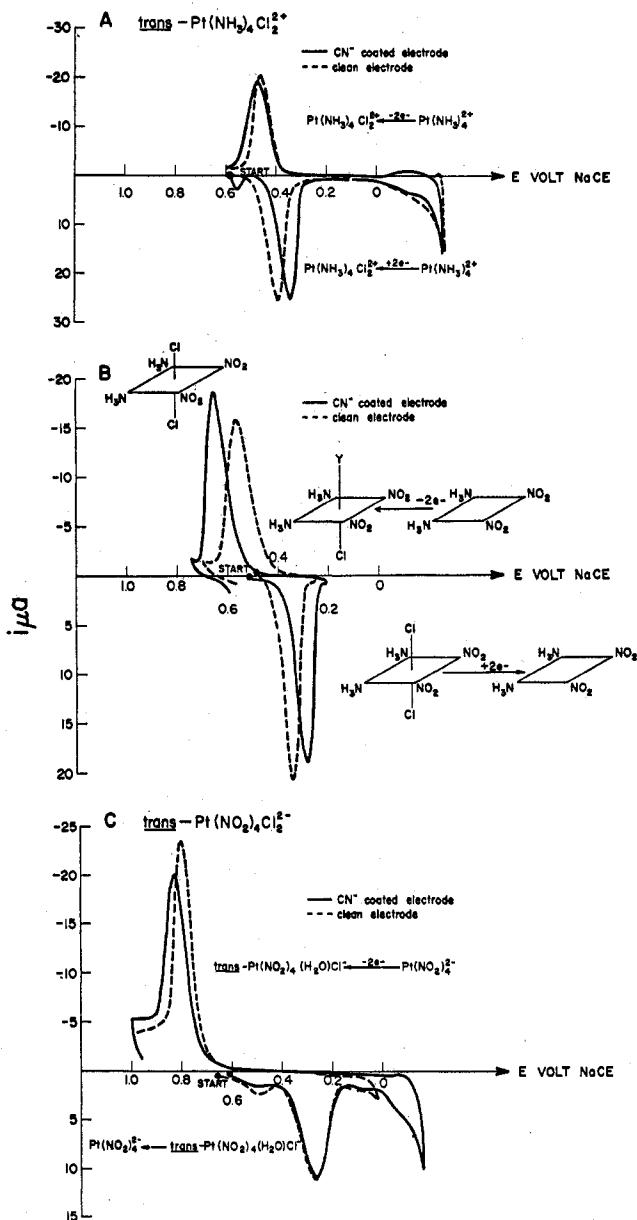

Figure 6.—Thin-layer current–potential curves for cationic, neutral, and anionic platinum complexes at CN-coated and clean platinum electrodes: curve A, 1 mF trans-[Pt(NH$_3$)$_4$Cl$_2$]Cl$_2$ + 10 mF NaCl + 1 F HClO$_4$; curve B, 1 mF cis,trans-Pt(NH$_3$)$_2$-(NO$_2$)$_2$Cl$_2$ + 10 mF NaCl + 1 F HClO$_4$; curve C, 1 mF trans-Pt-(NO$_2$)$_4$Cl$_2$ + 10 mF NaCl + 1 F HClO$_4$; solid curves, CN-coated electrode; broken curves, clean electrode. Experimental conditions were as in Figure 1, except that prior to recording the solid curve, the electrode was rinsed for 30 sec with 2 mF NaCN followed by thorough rinsing with water and with pure supporting electrolyte.

the *equatorial* bridged path. Neither Pt(C$_2$H$_4$)(H$_2$O)Cl nor the electrogenerated derivative Pt(C$_2$H$_4$)(H$_2$O)$_3$$^{2+}$ reacts by the axial (chloride ion accelerated) path. This may be the result of steric hindrance of the axial positions caused by the ethylenic protons in the complex. The observed sequence of current–potential curves can be understood in terms of the following reaction scheme. Oxidation of Pt(C$_2$H$_4$)(H$_2$O)Cl$_2$ proceeds according to eq 8; reduction of the resulting Pt(IV) product requires a bridging halide ligand and leads to its removal (eq 9). Pt(C$_2$H$_4$)(H$_2$O)$_3$$^{2+}$ is unreactive toward oxidation, apparently because the
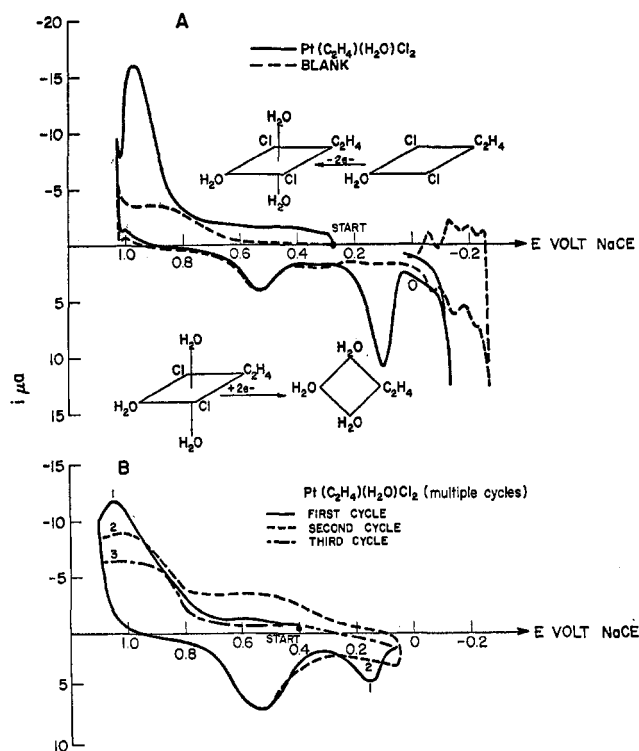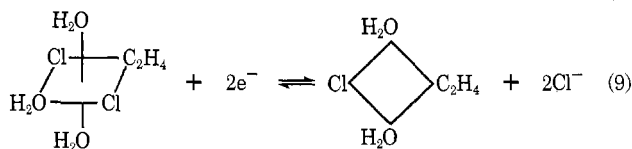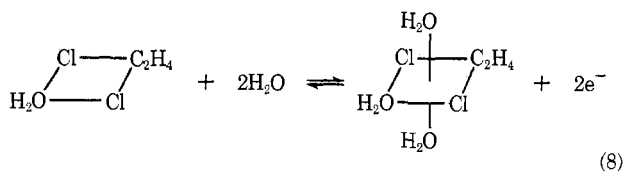
Figure 7.—Thin-layer current–potential curves for ethylene complexes of platinum: curve A, 1 mF KPt(C_2H_4)Cl_3^- + 10 mF NaCl + 1 F HClO$_4$; curve B, same solution composition as A; multiple scans.

$$\text{(8)}$$

$$\text{(9)}$$

ethylene ligand prevents oxidation *via* the axial bridge path and no halide ligands are available to serve in an equatorial bridge path.

Current–potential data for all of the platinum complexes studied in this work are summarized in Table I. The most immediate indication of the relative reaction rates can be gotten from the difference $_aE_p - _cE_p$ between anodic and cathodic peak potentials, large splittings corresponding to slow reactions.[2] Oxidation of Pt(II) complexes by way of the axial ligand bridge path, eq 2, follows eq 10[4] (please refer to the glossary at the end of this article for definitions of the symbols employed) when Y = Cl and eq 11 when Y = H$_2$O.

$$i = nFA \left(*k°_{23}\right)K\gamma\Gamma_{Cl}-C_{Cl}-C_{Pt(II)} \times$$

$$\exp\left[\frac{(1 - *\alpha_{23})F}{RT}(E - E°_{32})\right] \quad (10)$$

$$i = nFA \left(*k°_{23}\right)\gamma\Gamma_{Cl}-C_{Pt(II)} \times$$

$$\exp\left[\frac{(1 - *\alpha_{23})F}{RT}(E - E°_{32})\right] \quad (11)$$

Thus, the quantities on the left-hand side of eq 12 and

13 give a reasonably precise indication of the apparent reaction rate when Y = Cl or H$_2$O, respectively. The

$$*k°_{23} \exp\left[\frac{(1 - *\alpha_{23})F}{RT}(E - E°_{42})\right] =$$

$$\frac{i}{nFA Kk\Gamma_{Cl}-C_{Pt(II)}C_{Cl}-} \quad (12)$$

$$*k°_{23} \exp\left[\frac{(1 - *\alpha_{23})F}{RT}(E - E°_{42})\right] =$$

$$\frac{i}{nFA K\Gamma_{Cl}-C_{Pt(II)}} \quad (13)$$

formal standard potential $E°_{42}$ has been employed rather than the correct but inaccessible quantity $E°_{32}$; large relative errors are not likely to result since the free energies of activation on going from Pt(III) to Pt(II) or to Pt(IV) are probably relatively small. $E - E°_{42}$ will be assigned the value 0.2000 V, corresponding to the rising portion of the current–potential peak. Reduction of Pt(IV) complexes by the bridged path follows eq 14, and so the quantity shown in eq 15 will

$$i = nFA \left(*k°_{43}\right)C_{Pt(IV)} \exp\left[\frac{-*\alpha_{43}F}{RT}(E - E°_{43})\right] \quad (14)$$

$$*k°_{43} \exp\left[\frac{-*\alpha_{43}F}{RT}(E - E°_{43})\right] = \frac{i}{nFA C_{Pt(IV)}} \quad (15)$$

be tabulated as a measure of the relative reduction rate, with $E - E° = -0.200$ V.

Discussion

1. Oxidation of Pt(II) *via* the Axial Ligand Bridge Path.—Oxidation of Pt(II) complexes, not having halide ligands, in solutions containing halide ions appears to follow the axial ligand bridge path (eq 2). Association of potential ligands X and Y about the Pt(II) reactant as a prerequisite to electron transfer[2,4] is probably a consequence of the Franck–Condon principle: the activation energy for electron transfer is at a minimum when Pt(II) possesses a distorted octahedral structure intermediate between the structures of reactant and product in which the X and Y groups are located on opposite sides of the plane of the other four ligands. However, the species X, which is located between Pt(II) and the electrode, must be constituted so as not to prevent the complex from interacting with the high-field region at the interface (*i.e.*, it must be small, of suitable symmetry, and polarizable), since the field obviously provides the driving force for the reaction. The fact that only Cl$^-$, Br$^-$, and I$^-$ give clear-cut ligand-bridged acceleration of Pt(II) oxidation is thus probably an outgrowth of the Franck–Condon principle.

One halide is invariably added to the coordination sphere during oxidation but surprisingly the oxidation rate is not commonly observed to exhibit a linear dependence on halide concentration; this is an indication that the rate-limiting step involves interaction between *adsorbed* halide and the reactant complex, the interfacial excess of halide being close to the saturation amount and hence concentration independent at the positive potentials required for rapid Pt(II) oxidation. Since the halide-containing products commonly dis-

play a tendency toward hydrolysis, with eventual replacement of halide ligands by water, it is apparent that the halide-containing Pt(IV) complex obtained electrochemically is not simply the thermodynamically dictated product.

The decelerating influence of CN$^-$ ligands on Pt(II) oxidation can be attributed partly to stabilization of Pt(II) relative to Pt(IV) due to metal d $\rightarrow$ π^* back-bonding.[7,8] But this cannot be the sole explanation, for several reasons: the reported standard potentials indicate that Pt(II) complexes usually become easier to oxidize from a thermodynamic viewpoint as amine and halide ligands are replaced by CN$^-$ or SCN$^-$ in similar Pt(II)–Pt(IV) couples;[9,10] further, strictly speaking it is not the tabulated standard potentials but the inaccessible ones for the rate-limiting Pt(II)-to-Pt(III) step which should appear in the rate equations so that the significance of standard potentials for these rate processes remains uncertain in any event.[2] Finally, in the instances in which CN$^-$ ligands are thought to stabilize Pt(II) as compared to other ligands, shifts in standard potentials of less than about 120 mV are observed relative to similar complexes which undergo efficient oxidation at electrodes.

Experiments performed with complexes representative of the various structural and charge types indicate that although the species adsorbed from CN$^-$ or SCN$^-$ solutions noticeably influence the reaction rates, the effect is not large enough to account for the observed retardation in rate by CN$^-$ and SCN$^-$ ligands (for example, please see Figure 6).

Following the lines of recent publications by Pearson[10] and by Woodward and Hoffmann,[11] it appears that the preference of Pt(II) complexes for halide-bridged oxidation paths can be described in terms of the overlap of filled orbitals of the reactant complex with vacant orbitals of corresponding symmetry on the bridging group. The less rapid oxidation of Pt(II) complexes of CN$^-$ and SCN$^-$ can be attributed to stabilization of certain filled orbitals on the complex, namely, the potential "donor" orbitals in the initial electron-transfer step, due to interaction with π^* orbitals of the ligands.

Molecular interaction among the reactant complex, the ligand bridge, the molecular layer of solvent or other material in contact with the electrode, and the surface metal atoms is expected and observed to influence critically the outcome of the reactions. However, it appears practical to reserve the question of an experimentally tested molecular orbital description of the role of the molecular surface layer in the transition states of these reactions for discussion in future publications,[5,12,13] although certain points which are essential to the present discussion will be introduced here.

The rate of water exchange between the double layer and bulk solution has not been fully determined, but it
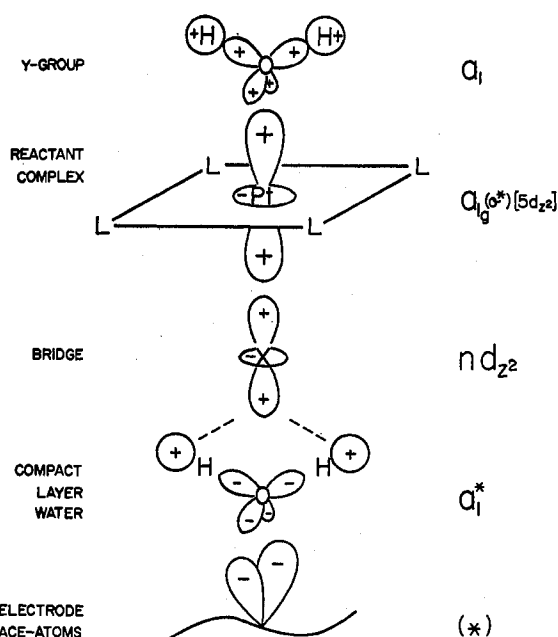

Figure 8.—Molecular orbital interactions leading to oxidation of Pt(II) by the axial bridge path.[18]

is at least clear from existing evidence[14,15] that water exchange is rather slow and that removal of water or its constituents from the compact layer is not necessarily a prerequisite of the electrode reactions presently under consideration. Thus, the electron-transfer intermediate may be interacting with the electrode either *through* or *around* the compact-layer water molecules and not necessarily at sites vacated by water. Since the population density of water molecules on the surface is expected and found[14] to be large, it seems reasonable to assume that electron transfer proceeds *through* the compact layer water (rather than around it), *in lieu* of more complete information on this point. Studies in which the compact layer is populated with species other than water not expected to be as well suited to electron transfer indicate that electrode rates depend critically upon compact-layer composition and in the direction expected on the basis of this assumption.[18] Direct interaction between the reactant or ligand bridge and the electrode surface will be discussed in more detail later.[5,18,15]

The molecular orbitals primarily responsible for normal bonding interactions among the reactants are not necessarily the only ones involved in the electron-transfer process, so that it is necessary to account for each effect separately, subject to the precondition that both sets of interactions be symmetry allowed under the same positioning of the nuclei. In particular, adsorption of the potential ligand bridge will be attributed to hydrogen bonding between the bridge and a molecule of the compact layer (for example, donation of electron density from two lobes of a chloride in tetrahedral hybridization toward the protons of a compact-layer water molecule). Interaction of the group Y (eq 2) with the Pt(II) reactant in the transition state is attributed to ion pairing (where appropriate) in combination with

(7) Yu. N. Kukushkin and S. Ch. Dkhara, *Russ. J. Inorg. Chem.*, **14**, 1483 (1969).

(8) I. I. Chernyaev, S. V. Zemskov, and B. V. Ptitsyn, *ibid.*, **10**, 1309 (1965).

(9) R. N. Goldberg and L. G. Hepler, *Chem. Rev.*, **68**, 229 (1968).

(10) R. G. Pearson, *Accounts Chem. Res.*, **4**, 152 (1971).

(11) R. B. Woodward and R. Hoffmann, "The Conservation of Orbital Symmetry," Verlag Chemie, Weinheim/Bergstrasse, 1970.

(12) G. M. Tom and A. T. Hubbard, University of Hawaii, unpublished experiments.

(13) M. A. Leban and A. T. Hubbard, University of Hawaii, unpublished experiments.

(14) J. W. Schultze, *Ber. Bunsenges. Phys. Chem.*, **73**, 483 (1969).

(15) W. Moats and A. T. Hubbard, University of Hawaii, unpublished experiments.
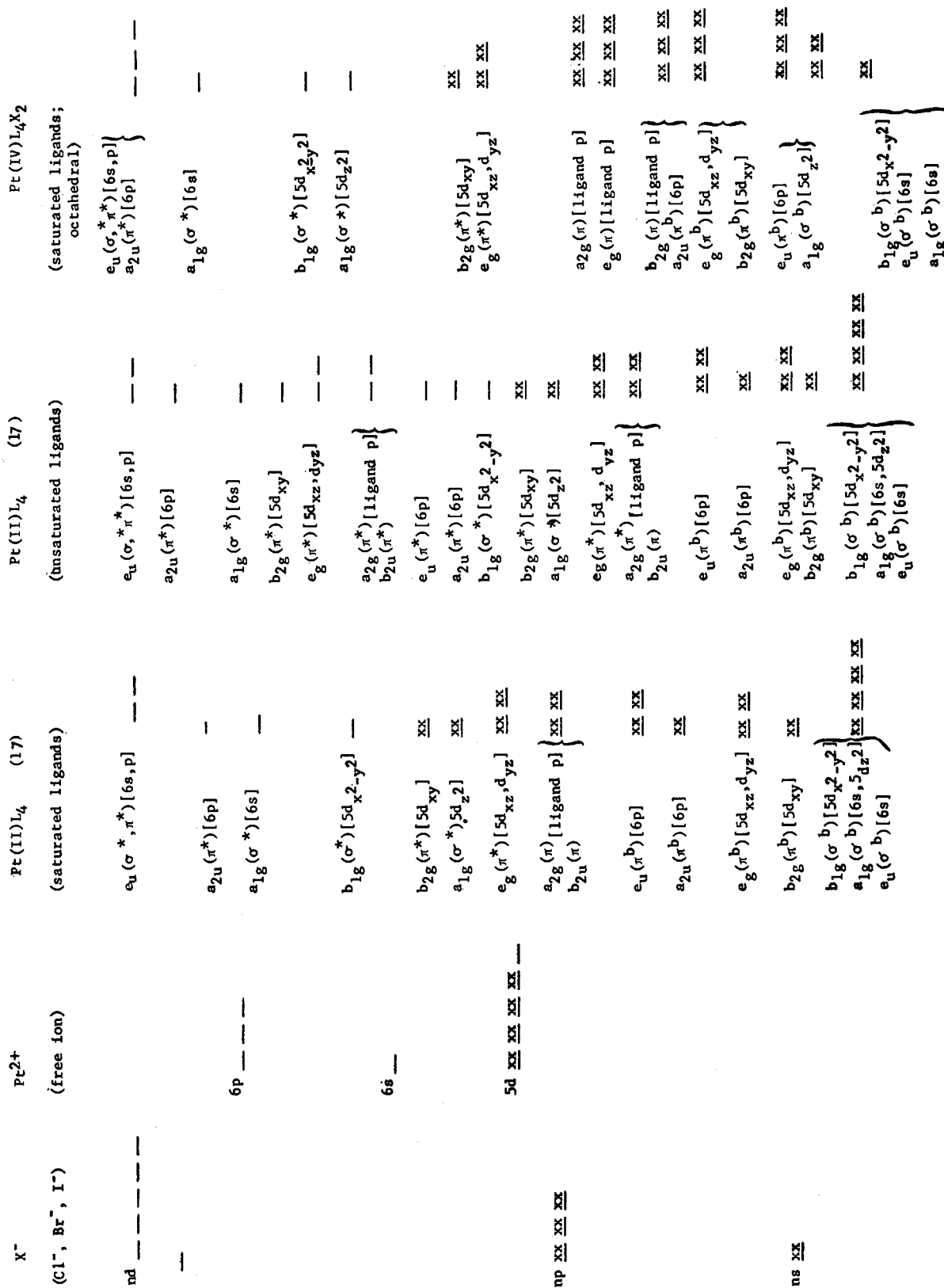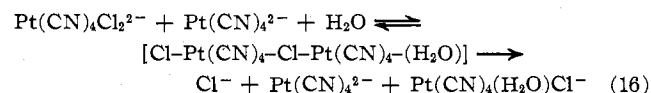
Column headers:

- X⁻ (Cl⁻, Br⁻, I⁻)
- Pt²⁺ (free ion)
- Pt(II)L₄ (17) (saturated ligands)
- Pt(II)L₄ (17) (unsaturated ligands)
- Pt(IV)L₄X₂ (saturated ligands; octahedral)

X⁻: np, ns

Pt²⁺ (free ion): $6p$, $6s$, $5d$

Pt(II)L₄ (saturated ligands):
$e_u(\sigma^*,\pi^*)[6s,p]$
$a_{2u}(\pi^*)[6p]$
$a_{1g}(\sigma^*)[6s]$
$b_{1g}(\sigma^*)[5d_{x^2-y^2}]$
$b_{2g}(\pi^*)[5d_{xy}]$
$a_{1g}(\sigma^*)5d_{z^2}$
$e_g(\pi^*)[5d_{xz},d_{yz}]$
$a_{2g}(\pi)[\text{ligand }p]$, $b_{2u}(\pi)$
$e_u(\pi^b)[6p]$
$a_{2u}(\pi^b)[6p]$
$e_g(\pi^b)[5d_{xz},d_{yz}]$
$b_{2g}(\pi^b)[5d_{xy}]$
$b_{1g}(\sigma^b)[5d_{x^2-y^2}]$
$a_{1g}(\sigma^b)[6s,5d_{z^2}]$
$e_u(\sigma^b)[6s]$

Pt(II)L₄ (unsaturated ligands):
$e_u(\sigma^*,\pi^*)[6s,p]$
$a_{2u}(\pi^*)[6p]$
$a_{1g}(\sigma^*)[6s]$
$b_{2g}(\pi^*)[5d_{xy}]$
$e_g(\pi^*)[5d_{xz},dyz]$
$a_{2g}(\pi^*)[\text{ligand }p]$, $b_{2u}(\pi^*)$
$e_u(\pi^*)[6p]$
$a_{2u}(\pi^*)[6p]$
$b_{1g}(\sigma^*)[5d_{x^2-y^2}]$
$b_{2g}(\pi^*)[5d_{xy}]$
$a_{1g}(\sigma\text{ }[5d_{z^2}]$
$e_g(\pi^*)[5d_{xz},d_{yz}]$
$a_{2g}(\pi^*)[\text{ligand }p]$, $b_{2u}(\pi)$
$e_u(\pi^b)[6p]$
$a_{2u}(\pi^b)[6p]$
$e_g(\pi^b)[5d_{xz},d_{yz}]$, $b_{2g}(\pi^b)[5d_{xy}]$
$b_{1g}(\sigma^b)[5d_{x^2-y^2}]$
$a_{1g}(\sigma^b)[6s]$
$e_u(\sigma^b)[6s]$

Pt(IV)L₄X₂ (saturated ligands; octahedral):
$e_u(\sigma^*,\pi^*)[6s,p]$
$a_{2u}(\pi^*)[6p]$
$a_{1g}(\sigma^*)[6s]$
$b_{1g}(\sigma^*)[5d_{x^2-y^2}]$
$a_{1g}(\sigma^*)[5d_{z^2}]$
$b_{2g}(\pi^*)[5d_{xy}]$
$e_g(\pi^*)[5d_{xz},d_{yz}]$
$a_{2g}(\pi)[\text{ligand }p]$
$e_g(\pi)[\text{ligand }p]$
$b_{2g}(\pi)[\text{ligand }p]$
$a_{2u}(\sigma^b)[6p]$
$e_g(\pi^b)[5d_{xz},d_{yz}]$
$b_{2g}(\pi^b)[5d_{xy}]$
$e_u(\pi^b)[6p]$
$a_{1g}(\sigma^b)[5d_{z^2}]$
$b_{1g}(\sigma^b)[5d_{x^2-y^2}]$
$e_u(\sigma^b)[6s]$
$a_{1g}(\sigma^b)[6s]$

Figure 9.—Qualitative molecular orbital energy level diagram for D_{4h} platinum complexes.

effects such as dispersion,[16] hydrogen bonding, and weak overlap between the a_{1g} (σ^*) [$5d_{z^2}$] orbitals of Pt(II) and filled orbitals of Y (typically, two lobes of an sp³ hybrid). Electron transfer then takes place between Pt^{II}Y and the adsorbed halide and is thought to proceed by interaction of the $a_{1g}(\sigma^*)$ orbitals of Pt^{II}Y with unfilled d orbitals such as nd_{z^2} of the bridging halide and interaction of these latter with unfilled levels such as the $a_1(\sigma^*)$ levels of a compact layer water molecule. A diagram illustrating the electron-transfer interactions in the transition-state complex appears in Figure 8. Qualitative orbital energy level diagrams for Cl⁻, Pt(II), and Pt(IV) are reproduced in Figure 9.[17]

Referring to Figure 9 it can be seen that the $a_{1g}(\sigma^*)$ levels of Pt(II) expected to participate in electron transfer are of lower energy in Pt(CN)$_4^{2-}$ than in PtCl$_4^{2-}$ due to the influence of the low-lying π^* levels of the CN⁻ ligands. Removal of an electron from these orbitals is, therefore, expected to proceed less readily for Pt(CN)$_4^{2-}$ than for PtCl$_4^{2-}$. This may be the effect which prompts the general slowness of oxidation of Pt(II) complexes containing unsaturated ligands. That complexes involving certain unsaturated ligands, such as the aromatic amines, exhibit normal reactivity is consistent with the suggestion that the ligand π^* levels involved in metal–ligand back-bonding are of relatively higher energy in such systems[18,19] and therefore stabilize the molecular orbitals of the complex to a lesser extent.

Evidence of extensive π back-bonding in Pt(CN)$_4^{2-}$ has been obtained from a number of sources. For instance, interpretation of pure quadrupole resonance spectra requires that the Pt–C bond length be assigned a value approaching that for a double bond.[20] Commonly accepted assignments of ultraviolet–visible transitions[17] were used to construct the energy level diagrams shown in Figure 9. The frequencies of the spectral bands in the far-infrared region attributable to Pt–C vibrational modes are not inconsistent with contraction of the Pt–C distance below that expected for a single bond.[21]

Rate data are not available for the oxidation of Pt(II) by homogeneous oxidizing agents. However, an indication of the trends to be expected can be gotten from consideration of the rates of ligand-substitution reactions of Pt(IV) complexes in halide solutions which are catalyzed by Pt(II); the reaction path apparently involves electron transfer between Pt(II) and Pt(IV) complexes with accompanying introduction of a ligand of a type not necessarily present in the Pt(IV) starting material. The reaction depicted in eq 16 is analogous

Pt(CN)$_4$Cl$_2^{2-}$ + Pt(CN)$_4^{2-}$ + H$_2$O $\rightleftharpoons$
  [Cl–Pt(CN)$_4$–Cl–Pt(CN)$_4$–(H$_2$O)] $\longrightarrow$
    Cl⁻ + Pt(CN)$_4^{2-}$ + Pt(CN)$_4$(H$_2$O)Cl⁻   (16)

to the electrochemical oxidation of Pt(CN)$_4^{2-}$ in chloride solution. The rate of this reaction is expected

(16) W. L. Masterton and T. Bierly, *J. Phys. Chem.*, **74**, 139 (1970).

(17) H. B. Gray and C. J. Ballhausen, *J. Amer. Chem. Soc.*, **85**, 260 (1963).

(18) C. Baker and D. W. Turner, *Proc. Roy. Soc., Ser. A*, **308**, 19 (1968).

(19) A. D. Baker, D. P. May, and D. W. Turner, *J. Chem. Soc., B*, 22 (1968).

(20) R. Ikeda, D. Nakamura, and M. Kubo, *J. Phys. Chem.*, **72**, 2982 (1968).

(21) Yu. Ya. Kharitonov, O. N. Evstaf'eva, I. B. Baranovskii, and G. Ya. Mazo, *Russ. J. Inorg. Chem.*, **14**, 248 (1969).

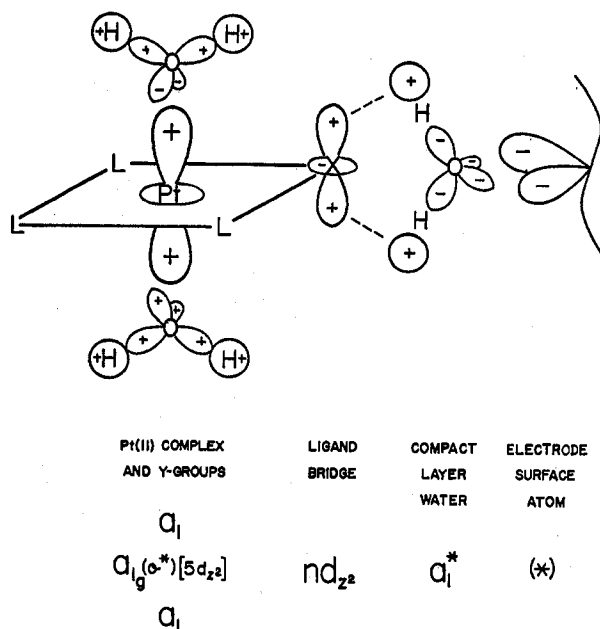| Pt(II) COMPLEX AND Y-GROUPS	LIGAND BRIDGE	COMPACT LAYER WATER	ELECTRODE SURFACE ATOM
a_1			
$a_{1g}(\sigma^*)[5d_{z^2}]$	nd_{z^2}	a_1^*	(*)
a_1			

Figure 10.—Molecular orbital interactions leading to oxidation of Pt(II) by the equatorial bridge path.[18]

and observed to be slower than for analogous complexes containing only saturated ligands.[22]

2. Oxidation of Pt(II) *via* the Equatorial Ligand Bridge Path.—Oxidation of Pt(II) complexes containing halide ligands by way of the equatorial ligand bridge path can be understood by a variation of the molecular orbital approach employed above for the axial bridge case. Occupied orbitals of the complex, such as $a_{1g}(\sigma^*)$ [$5d_{z^2}$], interact through the nd_{z^2} orbital of one halide ligand with unfilled orbitals of the compact layer (Figure 10). The slower reactivity of neutral and cationic complexes by the equatorial path than by the axial path probably stems to a great extent from the difficulty of bringing the groups Y (eq 3) sufficiently close to the complex for the Franck–Condon restriction to be met, to the lesser tendency of halide ligands than of ionic halide to adsorb at the interface, and to less favorable interaction between the $a_{1g}(\sigma^*)$ orbital of the complex and the nd_{z^2} orbital of the bridging ligand.

Cyanide ligands do not function as ligand bridges in the reactions of Pt(II) and Pt(IV). Thus, the slower reactivity of Pt(CN)$_4^{2-}$ than of PtCl$_4^{2-}$ by the equatorial bridge path is due at least in part to absence of potential bridging ligands from the coordination sphere. It would be of interest to study the oxidation of a Pt(II) complex containing similar numbers of both halo and cyano ligands. However, numerous attempts to prepare *cis*- and *trans*-Pt(CN)$_2$Cl$_2^{2-}$ yielded only an insoluble yellow material suspected to be polymeric.

3. Reduction of Pt(IV) *via* the Ligand Bridge Path.—The influence of an unsaturated ligand as a leaving group in the position trans to a single bridging halide ligand has been explored in a study of complexes of the type Pt^{IV}L$_4$XY (X = Cl, Br, I). Reduction of Pt^{IV}L$_4$XY proceeds rapidly to Pt^{II}L$_4$ when Y is a saturated ligand, but complexes in which Y = CN or SCN are reduced only slowly if at all (Figure 3). On the other hand, the identity of ligand L does not ap-

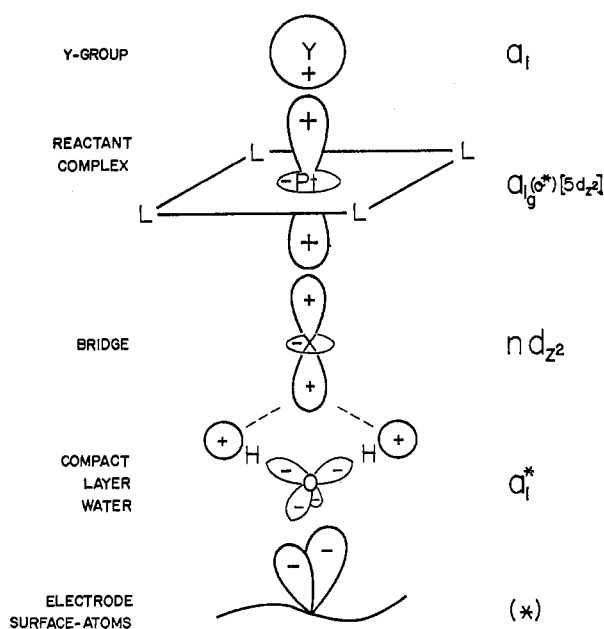(22) W. R. Mason, Jr., III, *Inorg. Chem.*, **9**, 1528 (1970).

Figure 11.—Molecular orbital interactions leading to reduction of Pt(IV).[13]

pear to be as critical. The presence of at least one halide ligand, X, is essential to facile reduction, of course.

Reduction of $Pt^{IV}L_4XY$ apparently proceeds through a halide-bridged transition state in which the highest unoccupied molecular orbital of the complex, $a_{1g}(\sigma^*)$, interacts with certain filled orbitals of the electrode surface through unfilled levels of the compact layer water and in turn through the unfilled nd_{z^2} orbital of the bridging halide ligand (Figure 11). A molecular orbital energy diagram for Pt(IV) complexes of D_{4h} symmetry is reproduced in Figure 9. Unsaturated ligands in positions labeled L are expected to stabilize the $a_{1g}(\sigma^*)$ level[17] and thus should increase the reaction rate slightly or leave it unchanged. This is in agreement with the observed result.

On the basis of the above conjecture, the unreactivity of complexes such as $Pt(CN)_5X^{2-}$ and $Pt(en)_2(CN)X^{2+}$ can be attributed to stabilization of the X–Pt–CN trans axis due to d–π^* back-bonding which renders more difficult the tetragonal distortion preceding electron transfer required in view of the Franck–Condon principle and which removes electron density from X thus decreasing the tendency of X to interact strongly with the interface.

Experimental Section

The theory and practice of electrochemistry with thin-layer cells has been reviewed recently[23] and equations of linear potential sweep voltammetry with thin-layer cells have been presented for typical reversible and irreversible cases.[24] Details of the experimental technique are described in recent publications dealing with platinum electrode kinetics,[2-4] although thin-layer techniques new to this work will be discussed below.

Perhaps it is worthwhile to summarize briefly the experimental equations, governing the reactions studied here. If a reaction of the form $Ox + ne^- \rightleftharpoons R$ proceeds reversibly, the peak potential equals the standard potential and the peak current depends only upon the n value and the experimental parameters (eq 17 and 18).

(23) A. T. Hubbard and F. C. Anson in "Electroanalytical Chemistry," Vol. 4, A. J. Bard, Ed., Marcel Dekker, New York, N. Y., 1970.
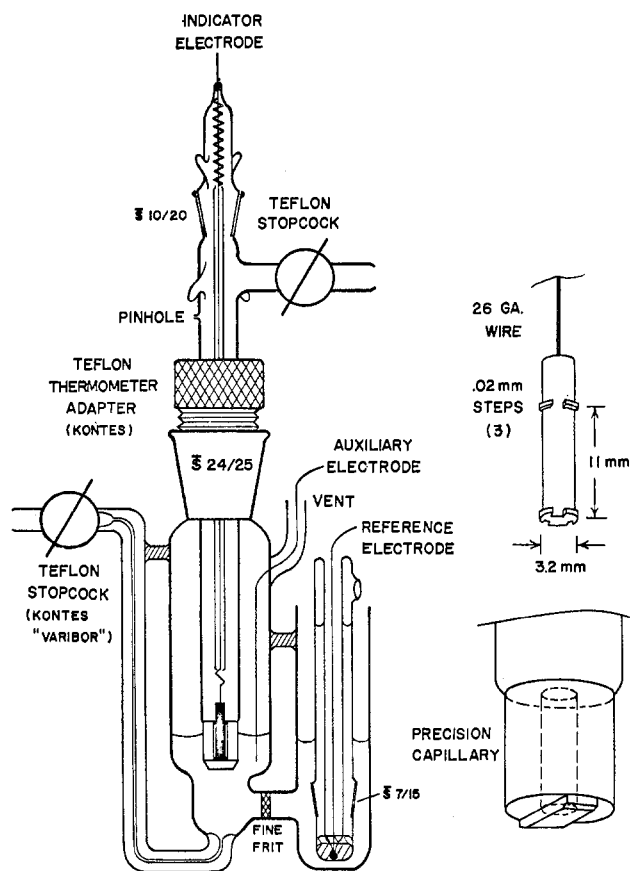(24) A. T. Hubbard, *J. Electroanal. Chem.*, **22**, 165 (1969).

Figure 12.—Thin-layer electrode and H cell.

$$_cE_p = E^\circ = {}_aE_p \tag{17}$$

$$_cI_p = \frac{n^2F^2(-r)VC^\circ}{4RT} = -{}_aI_p \tag{18}$$

On the other hand, the peak potential for an irreversible reaction is a measure of the rate constant of the reaction (eq 19 and 20). The peak current is indicative of the fraction of the

$$_cE_p = E^\circ + \frac{RT}{\alpha F} \ln\left[\frac{ARTk^\circ}{\alpha F(-r)V}\right] \tag{19}$$

$$_aE_p = E^\circ - \frac{RT}{(1-\alpha)F} \ln\left[\frac{ARTk^\circ}{(1-\alpha)FrV}\right] \tag{20}$$

applied voltage which is effective in lowering the activation energy of the reaction (eq 21 and 22). Slightly more detailed equations

$$_cI_p = \frac{\alpha nF^2V(-r)C^\circ_{Ox}}{eRT} \tag{21}$$

$$_aI_p = \frac{(1-\alpha)nF^2VrC^\circ_R}{eRT} \tag{22}$$

which allow for double-layer effects and which describe more complicated reaction paths are presented in ref 4.

The difference in potential between anodic and cathodic peak potentials is indicative of the rate of reaction—the larger the splitting the slower the reaction. α and k° reflect the influence of the electrical double layer; thus, for example, the cathodic peak current will be larger for cationic reactants than for anions, all else being equal; the opposite ordering will be observed for anodic reactions.[24]

The immersible thin-layer electrodes employed for this work (Figure 12) were constructed so that the platinum electrode could be removed from the glass container for cleaning and reinserted without undue contamination. The thin-layer cavity consisted of a precision Pyrex capillary (0.46-in. length × 0.1235-in. i.d.; Wilmad Glass Co., Buena, N. J. 08130) and a close-

fitting platinum rod (0.6-in. length $\times$ 0.1215-in. diameter, exclusive of steps near each end to ensure uniform positioning of the metal within the capillary).

Reproducible electrode surface pretreatment was accomplished as follows. The platinum electrode was removed from the glassware and heated to redness for 10 min in an oxidizing methane–oxygen flame, allowed to cool for a few seconds in air, and then inserted into the capillary. A cyclic current–potential curve was recorded in carefully deaerated 1 F HClO$_4$ from 0.6 to 1.3 to -0.3 and finally to $+0.4$ V *vs.* Na ce, which served the double purpose of removing the last traces of adsorbed organic materials and confirming the cleanliness of the surface. The surface was, of course, polycrystalline; experiments at single-crystal surfaces are in progress.[25]

All solutions were prepared from reagent grade chemicals. Triply distilled water was employed, the second distillation being from a solution of 10^{-3} F KMnO$_4$ in 10^{-3} F NaOH. Experiments were performed at 24 $\pm$ 1°. Potentials were measured relative to a calomel electrode made with 1 F NaCl (denoted "Na ce").

Table II lists the published procedure or other source of each platinum compound employed. Several of the compounds were obtained by new procedures, as follows.

trans-[Pt(en)$_2$(**CN**)Cl]Cl$_2$.—A 0.2-g amount of *trans*-[Pt(en)$_2$-Cl$_2$]Cl$_2$ was dissolved in a minimum of water; 2.0 g NaCN was then added in the form of a saturated aqueous solution. A trace of [Pt(en)$_2$]Cl$_2$ was also added as a catalyst. Within a few minutes, yellow crystals separated, which were collected by filtration.

The product was then dissolved in 1 ml of 1 F HCl and heated for 5 min near the boiling point; when the solution was chilled and added to 100 ml of 1:1 ethanol–ether mixture, a white powder was obtained in 50% yield. *Anal.* Calcd for [Pt(en)$_2$-(CN)Cl]Cl$_2$: C, 13.41; H, 3.58; N, 15.65; Cl, 23.77; Pt, 43.50. Found: C, 13.27; H, 3.62; N, 15.49; Cl, 23.62; Pt, 43.31.

Pt(en)(CN)$_2$.—A 0.2-g amount of Pt(CN)$_2$ (K & K Laboratories, Plainview, N. Y. 11803) was heated with an excess of pure ethylenediamine; the black solid which formed immediately was treated with 2 ml of H$_2$O. A white solid formed which was separated manually from a black by-product in about 50% yield and analyzed. *Anal.* Calcd for Pt(en)(CN)$_2$: C, 15.60; H, 2.60; N, 18.25. Found: C, 15.63; H, 2.51; N, 18.50.

trans-Pt(NH$_3$)$_2$(**CN**)$_2$.—A 0.3-g amount of *trans*-Pt(NH$_3$)$_2$Cl$_2$ was treated with exactly 2 mol of AgNO$_3$ per mole of platinum and 1 ml of H$_2$O. The mixture was heated for 5 min and filtered. To the filtrate was added 2 mol of KCN per mole of platinum. The product, a white solid, formed immediately and was collected in 56% yield.[26] *Anal.* Calcd for Pt(NH$_3$)$_2$-(CN)$_2$: C, 8.50; H, 2.13; N, 20.00. Found: C, 8.27; H, 2.20; N, 19.72.

(25) A. T. Hubbard, University of Hawaii, unpublished experiments.

(26) S. Ch. Dkhara, M. I. Gel'fman, and Yu. N. Kukushkin, *Russ. J. Inorg. Chem.*, **13**, 1307 (1968).

trans-[Pt(en)$_2$(SCN)Cl](NO$_3$)$_2$.—Equimolar quantities of LiSCN and HCl were added to 0.1 g of [Pt(en)$_2$(OH)$_2$](NO$_3$)$_2$ dissolved in a minimum of water. The mixture was allowed to stand overnight at room temperature, after which a slight excess of concentrated HNO$_3$ was added to the solution. Due to its high solubility the product was not isolated from solution.

List of Symbols

A	Electrode area, cm^2
α_{43}	Charge-transfer coefficient of a Pt(IV)–Pt(III) couple, etc.
*	Indication of an empirical value
C_N	Concentration of species N
$C°_N$	Initial concentration of species N
$E°_{43}$	Formal standard potential of a Pt(IV)–Pt(III) couple, etc.
$_aE_p$, $_cE_p$	Peak potential of positive- or negative-going current potential (cp) curve, respectively
F	Faraday constant, 96,493 C equiv^{-1}
Γ_{Cl^-}	Interfacial excess of Cl$^-$ in the compact double layer mole, cm^{-2}
$_aI_p$, $_cI_p$	Peak current of positive- or negative-going cp curve, respectively
K	Equilibrium constant, [Pt^{II}L$_4$X]/[Pt^{II}L$_4$][X$^-$]
$k°_{43}$	Standard electrochemical rate constant of a Pt(IV)–Pt(III) couple, etc., cm sec^{-1}
γ	Parameter, cm^{-1}, reflecting approximate proportionality between Γ_{Cl^-} and surface activity of chloride ion
n	Number of electrons transferred per molecule
r	Velocity of potential sweep, V sec^{-1}
V	Volume of the thin-layer electrode cavity, cm^3
Na ce	Denotes calomel reference electrode prepared with 1 F NaCl